Separation Science and Technology
Publication details, including instructions for authors and subscription information:
http://www.informaworld.com/smpp/title~content=t713708471

A Study on the Preparation and Gas Permeation of Porous Alumina Supports

Ting-Chia Huang[a]; Huey-Ing Chen[a]
[a] DEPARTMENT OF CHEMICAL ENGINEERING, NATIONAL CHENG KUNG UNIVERSITY TAINAN, TAIWAN, REPUBLIC OF CHINA

To cite this Article Huang, Ting-Chia and Chen, Huey-Ing(1995) 'A Study on the Preparation and Gas Permeation of Porous Alumina Supports', Separation Science and Technology, 30: 10, 2189 — 2209
To link to this Article: DOI: 10.1080/01496399508013901
URL: http://dx.doi.org/10.1080/01496399508013901

SEPARATION SCIENCE AND TECHNOLOGY, 30(10), pp. 2189–2209, 1995

A Study on the Preparation and Gas Permeation of Porous Alumina Supports

---

TING-CHIA HUANG and HUEY-ING CHEN
DEPARTMENT OF CHEMICAL ENGINEERING
NATIONAL CHENG KUNG UNIVERSITY
TAINAN, TAIWAN 70101, REPUBLIC OF CHINA

ABSTRACT

The preparation and gas permeation of porous alumina supports were studied. The influences of the amount of PVA on the properties of the alumina slips, microstructure of the supports, and gas permeation were investigated. The experimental results show that the addition of PVA in the preparation process is useful for controlling the porosity of the supports without significantly changing other microstructural properties. Permeation measurements of H_2, He, CH_4, N_2, O_2, and CO_2 showed that gas transport through various supports under low transmembrane pressures (100–220 kPa) at room temperature (26.5°C) was in the transition region, which combined the Knudsen diffusion and Poiseuille flow. The average radii of active pores for the supports, calculated from the gas permeability method, were compared with those measured by mercury porosimetry. The porosity–tortuosity factors and the tortuosity factors of the supports were also estimated and are discussed.

INTRODUCTION

The use of ceramic membranes has developed rapidly in recent years owing to their excellent advantages: high thermal, chemical, biological, and structural stability, and good catalytic properties. A ceramic membrane usually consists of a coarse-pore ceramic support and one or more fine-pore layers. The support should be mechanically strong and offer good permeability. Porous media with pores from about 100 nm to a few microns have been widely used in a variety of applications such as microfiltration and in supporting materials for ultrafiltration, gas separation, pervaporation, and catalytic membranes.

The slip casting of alumina supports requires the addition of binders to provide adequate green strength. Polyvinyl alcohol (PVA) was selected as a binder for this work because it is readily available and widely used in ceramic processing (1). Numerous articles related to the preparation and characterization of the permselective top layer of alumina membranes have been published in recent years (2–9). Also, the fabrication of supporting media has been commercialized and is well developed. However, very few studies (10) have been conducted on investigating the effects of PVA amounts on microstructure and gas permeability of ceramic supports prepared with PVA as a binder.

The microstructural properties of a porous medium (pore size, pore size distribution, surface area, and porosity) depend on the preparation methods. Porous structures are too complex to be represented by a single number or even by one simple model. The internal geometries of a porous medium are poorly understood, and thus a so-called *tortuosity factor* τ is used to account for mass transfer through a porous medium. The tortuosity factor is an empirical coefficient accounting for the random orientation of pores in a material. For a porous medium with a uniform pore size distribution, the tortuosity factor is $1 < \tau < \infty$. However, the tortuosity factor can be less than unity when there are two or more types of pores in a structure (11).

The evaluation of pore size and size distribution of active pores in porous media is important for the preparation of membranes and an understanding of gas permeability/diffusion mechanisms in porous media. There are a number of methods for measuring pore sizes and their distribution in porous media, e.g., gas adsorption–desorption, mercury porosimetry, and thermoporometry. These methods are capable of providing information on average pore size, pore size distribution, porosity, and specific surface area. However, they are not able to discriminate between "active" and "passive" pores (12). For many applications, such as gas separation, only the active pores are important, and a narrow size distribution of active pores is essential. A recently developed dynamic flow technique (permporosimetry) (13–15) allows determination of the pore size distribution of the supported top-layer or of the modified layer of ceramic membranes. This method is based on measurements of the flow rate of a gas mixture consisting of a noncondensable gas and a condensable gas through a membrane as a function of the vapor pressure of the condensable gas. However, this method is specific to the active pores of a UF membrane or in the dense layer of the membrane, and is insensitive to the pores in the supporting porous medium. The gas permeability method (16–18) is remarkable in its simplicity for measuring the average size of the active pores in porous media. The method is based on measurements of the flow rate of a pure, nonadsorbable, and noncondensable gas through a porous medium as a function of the pressure drop across the medium.

In the present work, the influences of the amount of PVA in the preparation, the microstructure, and the gas permeation properties of alumina supports are investigated. Furthermore, the pore structures of various supports as determined by the gas permeability method and mercury porosimetry are compared and discussed.

THEORETICAL

In pressure-driven gas separation processes via porous media, the transport mechanism mainly includes Knudsen diffusion and Poiseuille flow.

The relative contribution of Knudsen diffusion to the Poiseuille flow on the overall transport rate depends on the Knudsen number, Kn, which is defined as the ratio of mean free path (λ) of the gas to the pore radius (r) of the medium, and is described by (10, 11, 19)

$$\mathrm{Kn} = \lambda / r \tag{1}$$

When the gas density is low, or if the pores are quite small, or both (i.e., $\mathrm{Kn} \gg 1$), the molecules collide with the pore wall much more frequently than with each other. This is known as "Knudsen diffusion" or "Knudsen flow." The molecules hitting the wall are adsorbed and then reflected in random directions. Therefore, the gas flux is reduced by the wall resistance due to the diffusion, reflection, and adsorption of molecules.

If the Knudsen number is much smaller than unity, the Poiseuille flow mechanism is dominant. This means that the molecules collide at least as much with each other as with the pore wall, and the momentum loss is progressively and smoothly transferred to the bulk of the gas.

The transition region of gaseous flow occurs mainly in the range $0.01 < \mathrm{Kn} < 10$ (20). The flux of gas through a porous medium in this regime can be expressed by the following equations (21–24):

$$J = F_0 \frac{\Delta P}{l} \tag{2}$$

and

$$F_0 / l = F_{0K} + F_{0P} P_{\mathrm{ave}} \tag{3}$$

in which

$$F_{0K} = 1.064 \frac{1}{l} \frac{\epsilon}{\tau} \frac{r}{(RTM)^{0.5}} \tag{4}$$

and

$$F_{0P} = \frac{1}{8\eta RTl} \frac{\epsilon}{\tau} r^2 \tag{5}$$

where J is the flux, F_0/l is the permeability, ΔP is the transmembrane pressure, P_{ave} is the average pressure across the porous medium, ϵ is the porosity, τ is the tortuosity, l is the thickness of the porous medium, T is the operating temperature for permeation, M is the molecular mass of pure gas, and R is the gas constant.

The first term on the right-hand side of Eq. (3) is contributed by Knudsen diffusion, and the second term is due to Poiseuille flow. As can be seen from Eqs. (4) and (5), Poiseuille flow is nonseparative, while gas separation by the Knudsen diffusion can be determined from the ratio of permeabilities of the two gases, A and B, and is limited by the square root of the ratio of molecular masses:

$$\frac{F_{0K,A}}{F_{0K,B}} = \sqrt{\frac{M_B}{M_A}} \tag{6}$$

A plot of $J/\Delta P$ as a function of the average pressure P_{ave} should be a straight line. The value of F_{0P} is obtained from the slope of this line, and the value of F_{0K} is obtained by extrapolation of permeability data to zero pressure. The ratio $F_{0P}P_{ave}/F_{0K}$ reflects the relative importance of Poiseuille flow and Knudsen diffusion in the separation process.

By dividing the Poiseuille permeability F_{0P} by the Knudsen permeability F_{0K}, Eq. (7) is obtained:

$$\frac{F_{0P}}{F_{0K}} = \frac{r}{8.512\eta} \left(\frac{RT}{M}\right)^{-0.5} \tag{7}$$

and the average radius of the "active" pores for a porous medium can be estimated by

$$r = 8.512\eta \left(\frac{RT}{M}\right)^{0.5} \frac{F_{0P}}{F_{0K}} \tag{8}$$

Equation (8) indicates that the average radius of the active pores can be calculated from the pressure dependence of gas permeabilities of a porous support without further estimation of porosity ϵ and tortuosity factor τ. Moreover, according to Eqs. (4) and (5), the terms of $F_{0K}\sqrt{MT}$ and $F_{0P}RT\eta$, which are independent of operating temperature and the nature of the gas, are characteristics of a porous structure. Substituting the average radius of active pore r obtained from Eq. (8) into Eq. (4) or (5), the porosity–tortuosity factor (ϵ/τ) and tortuosity factor (τ) of the porous support can thus be estimated.

EXPERIMENTAL

Materials

α-Al_2O_3 (Showa Denko Co.) and γ-Al_2O_3 (Merck Co.) powders were used as the starting materials for preparation of the supports. Polyvinyl alcohol, PVA (DP = 500, obtained from Fluka Chemicals Co.), and diammonium hydrogen citrate (Ferak Co.) were used as additives. All of the above chemicals were GR grade. Gypsum powders purchased from Maruishi Gypsum Co. were used to prepare the molds. Water used in the reactions was deionized using a two-stage Milli-QSP water purification system (Millipore Corp.).

Preparation Procedure

Preparation of Alumina Slip

(1) α-Al_2O_3 powders as material: Two hundred grams of α-Al_2O_3 powders were added to 200 g aqueous solution which dissolved a specific amount of PVA and diammonium hydrogen citrate. Then, by using 2 kg of Al_2O_3 balls (ϕ2 cm), the slurry was milled for 5 hours. After removal of air bubbles by vacuum suction, the alumina slip was obtained. (2) γ-Al_2O_3 powders as material: The procedure used for the preparation of γ-alumina slip was similar to that proposed by Leenaars and Burggraaf (25). Two hundred grams of γ-Al_2O_3 powders and a proper amount of 1.6 N HNO_3 solution (Al_2O_3/HNO_3 molar ratio = 1:0.03) were mixed in a ball-mill to prepare an alumina slip. The time for milling was 20 hours.

Preparation of Alumina Supports

The slip-casting process was used for the preparation of alumina supports. The degassed alumina slip was poured into PMMA rings (ϕ6.6 cm) which were placed on a gypsum mold. Water was rapidly absorbed by the gypsum, and subsequently the gels were separated from the mold. After drying, the α-alumina supports were obtained by firing the α- and γ-Al_2O_3 gels under different procedures. The α-Al_2O_3 gels were calcined with a heating rate of 3°C/min to 600°C, held for 1 hour to burn out the

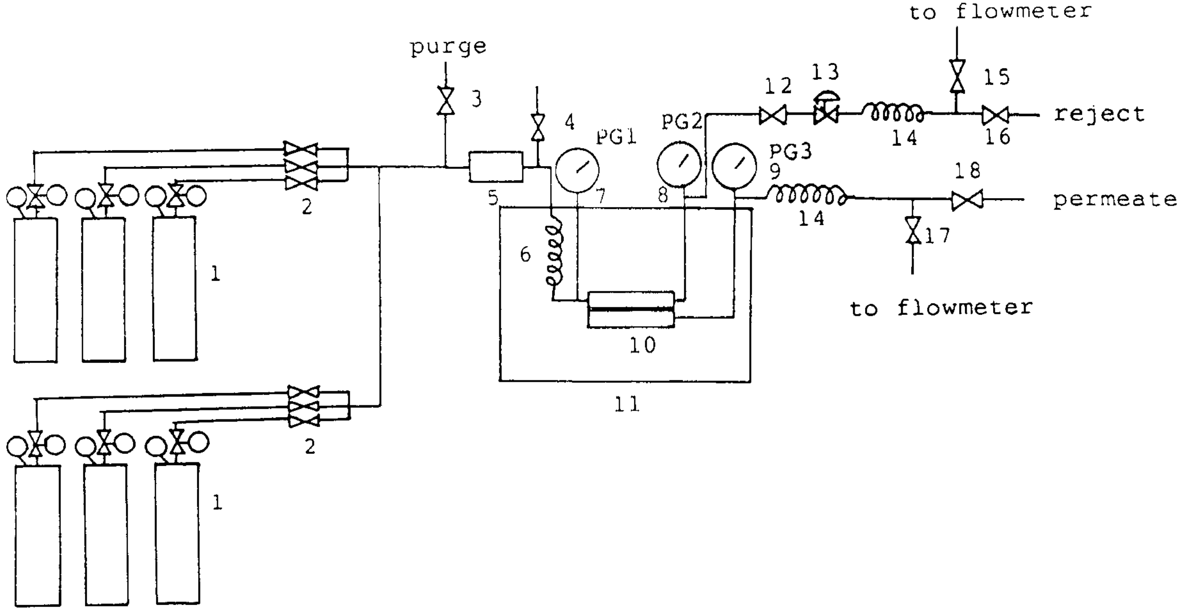

FIG. 1 Schematic diagram for gas permeation experiments: (1) gas cylinder, (2, 3, 4, 12, 15, 16, 17, 18) valves, (5) mass flow controller, (6) preheating coil, (7, 8, 9) pressure gauges, (10) permeator, (11) oven, (13) backpressure regulator, (14) cooling coil.

additives, and then raised to 1100°C with a heating rate of 3°C/min and finally held for 1 hour. The calcined gels were trimmed, burnished, cleaned, dried, and then sintered at 1350°C for 1 hour. In a different procedure, the γ-Al_2O_3 gels were sintered to 1350°C with a heating rate of 10°C/min, held for 16 hours, and then the the surface of the gels was finished. During this firing process the gels had been transformed into an α-phase as could be confirmed by x-ray diffraction measurement.

Permeation of Gases

A stainless-steel permeation cell with a flat circular support clamped between two pieces of silicon rubber was placed in a thermostat chamber. The effective permeation area of the support was 18.6 cm^2. The thickness of the support used in this work was within 1–2 mm. A schematic representation of the gas permeation apparatus is illustrated in Fig. 1. The permeation characteristics of H_2, He, CH_4, N_2, O_2, and CO_2 through three supports denoted BM-26 (PVA 1%), BM-23 (PVA 5%), and BM-24 (PVA 10%) were studied in this work. The upstream pressure was controlled by the regulator of the gas cylinder, and the gas downstream was vented to air. The fluxes of permeate gases were measured by a soap-bubble flowmeter at room temperature (i.e., 26.5 ± 0.5°C) and a transmembrane pressure range of 100 to 220 kPa.

Characterization

The surface area of the support was measured by the nitrogen adsorption–desorption method using nitrogen gas with a Micromeritics ASAP 2000 system. The porosity, pore size, and pore size distribution analysis was carried out with a mercury porosimeter (Micromeritics Autopore II-9220 system). The viscosity of an alumina slip was measured by a programmable rheometer (Model DV-III, Brookfield Co.). X-ray diffraction studies were performed with a Rigaku RX-III x-ray diffractometer with Ni-filtered CuKα radiation. A Jeol JXA-840 scanning electron microscope was used for scanning the surface morphology of the support.

RESULTS AND DISCUSSION

Effect of PVA on the Properties of Alumina Slip

Figure 2 showed the pH change of alumina slips with various amounts of PVA before and after the milling process. The pH values for various solutions without adding Al_2O_3 powder were all about 5.8. The pH value suddenly raised to about 8.8 when the Al_2O_3 powder was added and then increased with increasing milling time due to the adsorption of hydrogen

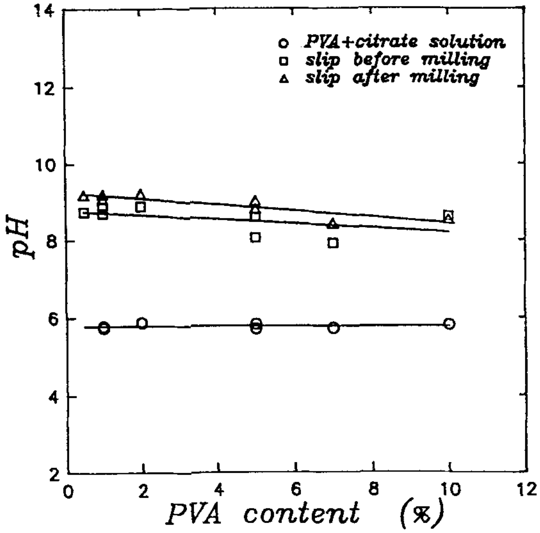

FIG. 2 The pH change of alumina slips in the milling process.

ions (26–28). The final pH value approached a constant value of 9.2 independent of the amount of PVA. After milling, a well-dispersed slip was obtained.

The viscosities of the stable slips were strongly affected by the amounts of PVA added during the preparation of alumina slips. As shown in Fig. 3, the viscosity of the slip was low and behaved as a Newtonian fluid when the PVA content was below 2%. When the PVA content was above 5%, the viscosity of the slip increased significantly and the rheological behavior was that of a plastic fluid.

In fact, colloid dispersions in this system are stabilized by a combination of electrostatic repulsion due to the adsorbed hydrogen ion at the particle surface and the steric effects arising from solvated polymer attached to the particle (29). In the case of a slip with a low concentration of polymer (e.g., below 2% PVA), the polymer is probably adsorbed on the particles by multipoint anchoring, and the rheology of the deflocculated dispersion becomes near-Newtonian. When the amount of PVA is increased, the polymer is forced to attach to the particle surface with a few segments in tails (or loops). In this situation the interpenetration of polymers between particles frequently increases the flow resistance of the dispersion and leads to high viscosity. When the shear rate is raised, the aggregates break

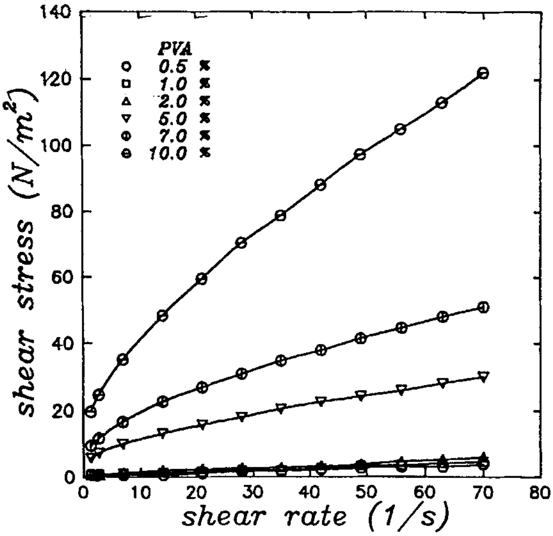

FIG. 3 The viscosities of alumina slips with various amounts of PVA.

down and the viscosity of the slip decreases subsequently, as shown in Fig. 3 (30, 31).

Effect of PVA on the Microstructural Properties of Alumina Supports

The pore size distributions for various supports with different amounts of PVA are illustrated in Fig. 4. The median pore diameters and surface areas for various supports are indicated in Fig. 5. Figure 6 shows the dependences of pore volume and porosity of the supports on the PVA amounts. It is found that the median pore diameter and the shape of pore size distribution of the supports underwent no significant change with varying PVA amounts, while the pore volume and porosity of the supports consistently increased with an increase of PVA amounts. Figure 7 illustrates the tendency of a larger void volume for support when the amount of PVA is increased. In the presence of polymer, as mentioned above, the distance between dispersed particles of a slip increases with the amount of PVA because of the steric effect. However, the median pore diameter and the shape of pore size distribution of alumina supports prepared with various amounts of PVA were quite similar after the firing process.

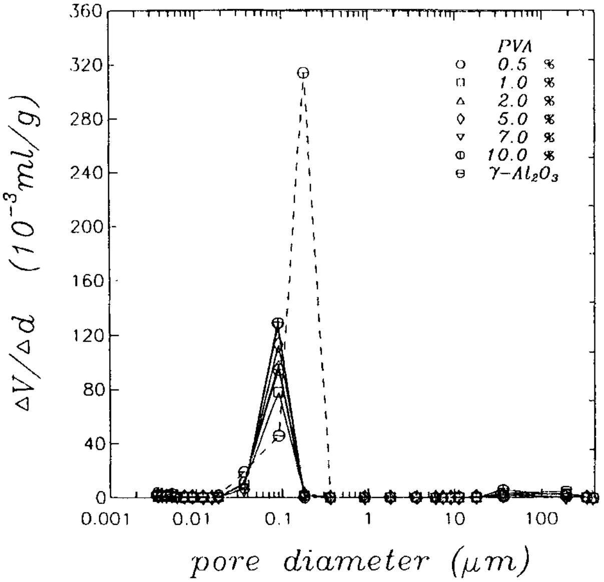

FIG. 4 Pore size distribution of various supports.

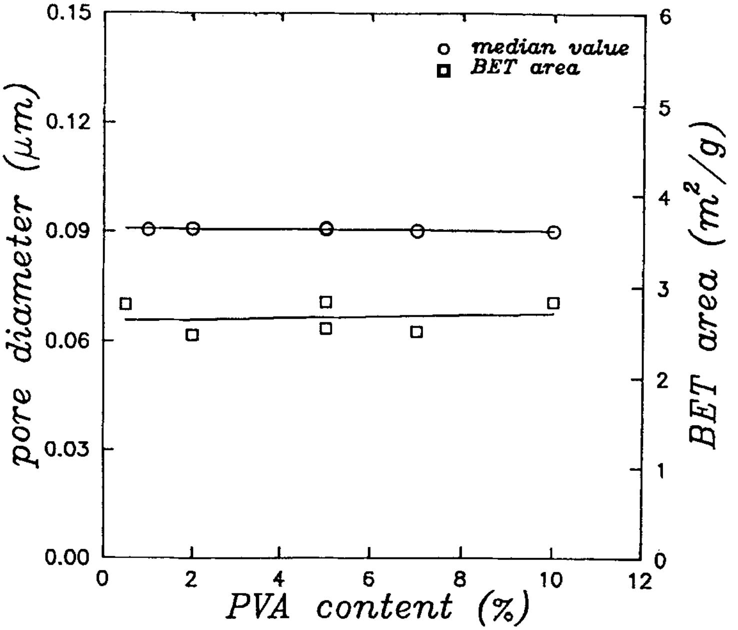

FIG. 5 Median pore diameter and surface area for various supports.

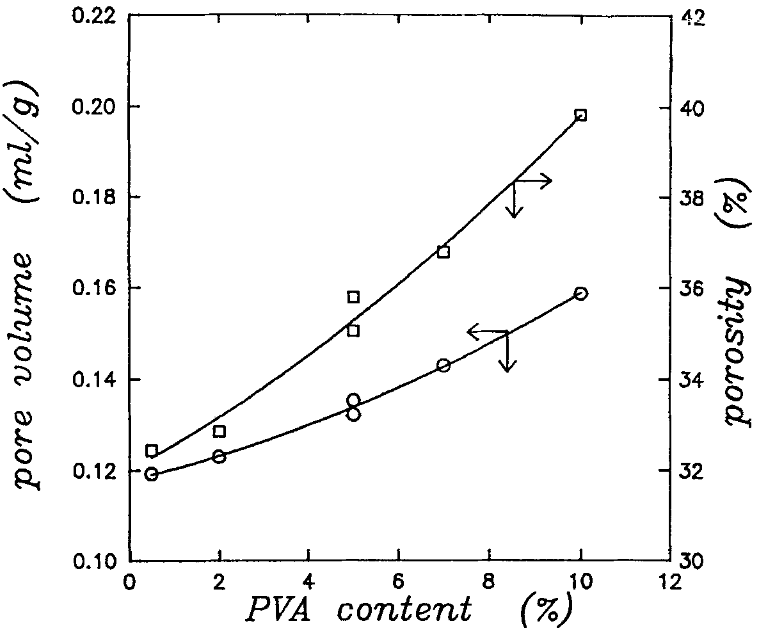

FIG. 6 Pore volume and porosity for various supports.

From these results it can be concluded that the addition of PVA not only plays a role as a binder and colloid stabilizer, but it also may control the porosity of supports without changing the other microstructural properties significantly.

Transport Mechanism of Gas Permeation through the Porous Supports

The fluxes of H_2, He, CH_4, N_2, O_2, and CO_2 through the three alumina supports BM-26, BM-23, and BM-24 were linearly proportional to the transmembrane pressure. The dependences of gas permeabilities (F_0) on the average pressure through the three supports showed linear relationships as illustrated in Figs. 8, 9, and 10, respectively. Based on these plots, the rate of gas transport through BM-24 (PVA 10%) is the fastest among the three supports. The values of F_{0K} and F_{0P} were obtained from the intercepts and slopes of these linear plots, as listed in Table 1. Since the Knudsen numbers of gaseous flow through these supports under the experimental conditions are mostly in the 0.01 to 10 range, the transports

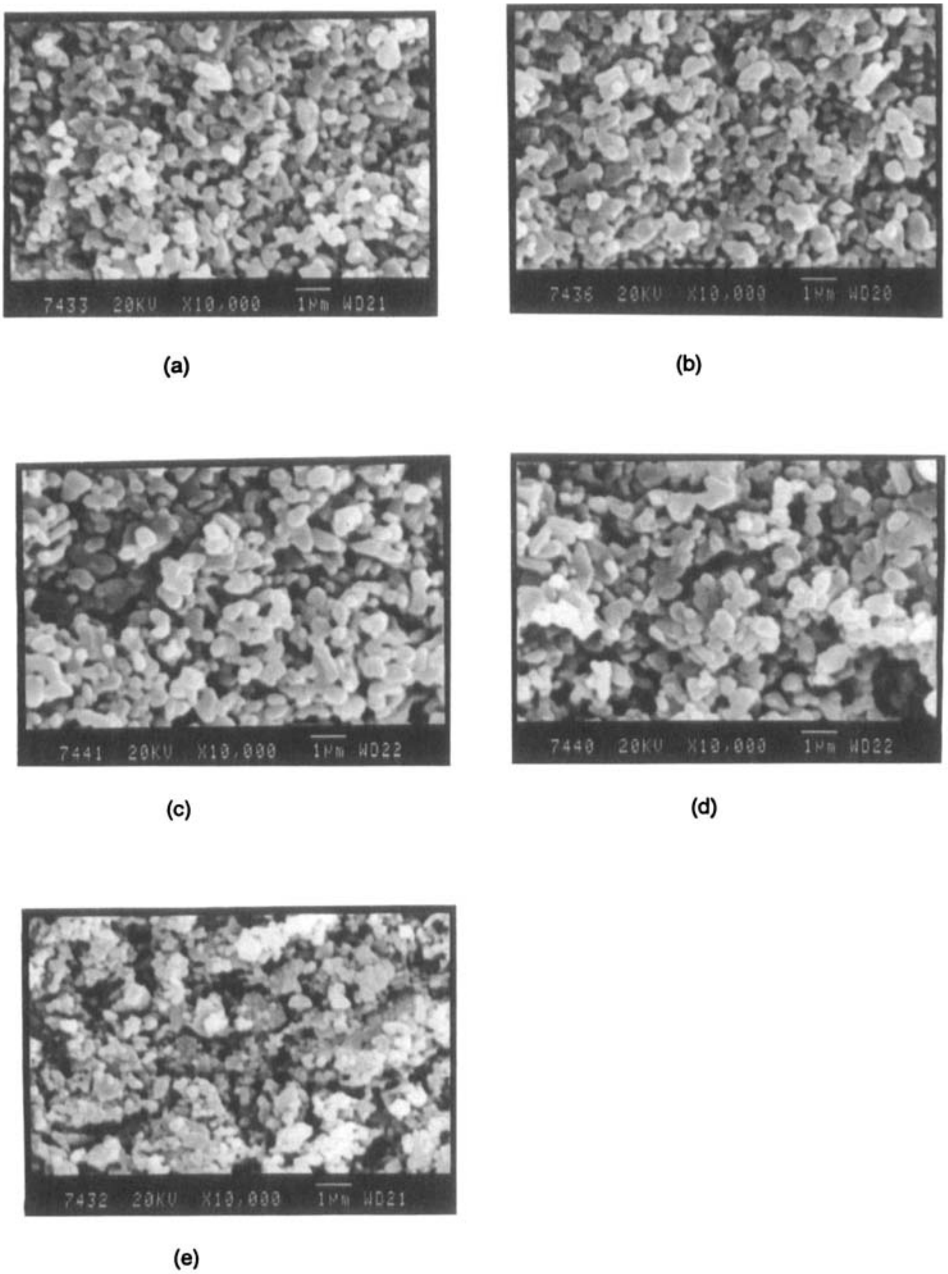

FIG. 7 Scanning electron micrographs for various supports. (a) BM-25, PVA 0.5%; (b) BM-26, PVA 1%; (c) BM-23, PVA 5%; (d) BM-24, PVA 10%; (e) BM-32, prepared from γ-Al_2O_3 powder.

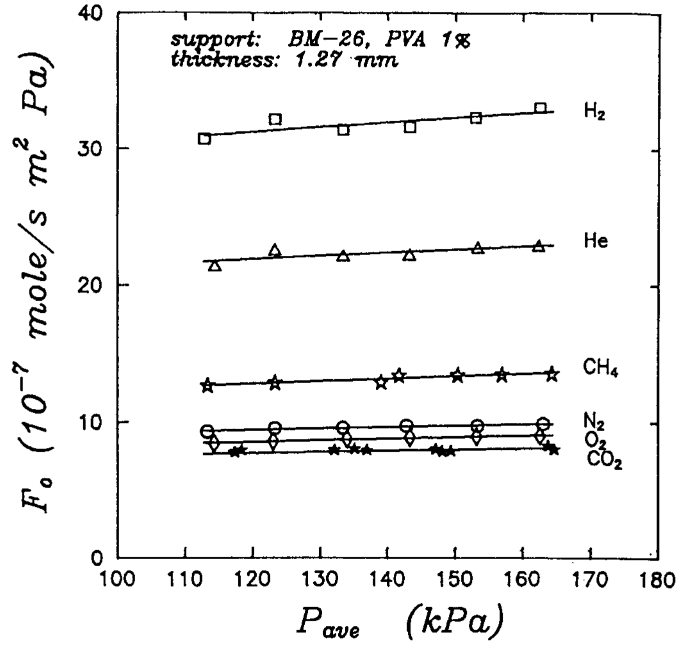

FIG. 8 Plot of F_0 vs P_{ave} at 26.5°C through the support prepared with 1% PVA.

of gases are in the transition region, i.e., the flux is governed by both Knudsen diffusion and Poiseuille flow.

To verify that the values obtained from the intercepts of these lines should be attributed to the Knudsen diffusion only, the dependence of $F_{0K}\sqrt{MT}$ on the molecular mass of gas for each support was plotted. A nearly horizontal line was found, as shown in Fig. 11. It was realized that the values of $F_{0K}\sqrt{MT}$ are independent of the molecular mass of gas, and therefore the permeability is clearly due to Knudsen diffusion only, as seen in the first term on the right-hand side of Eq. (3). The results in Table 1 also show that Knudsen diffusion played an important role in the transport rate of all six gases, including CH_4 and CO_2 which are condensable in the porous media. Consequently, the six gases used in this study were considered to be nonadsorbable and noncondensable under the conditions tested.

Estimation of Porosity–Tortuosity Factors and Tortuosity Factor for the Alumina Supports

The characterization of a porous support for separation purposes, however, is aimed at predicting the transport properties and separation effi-

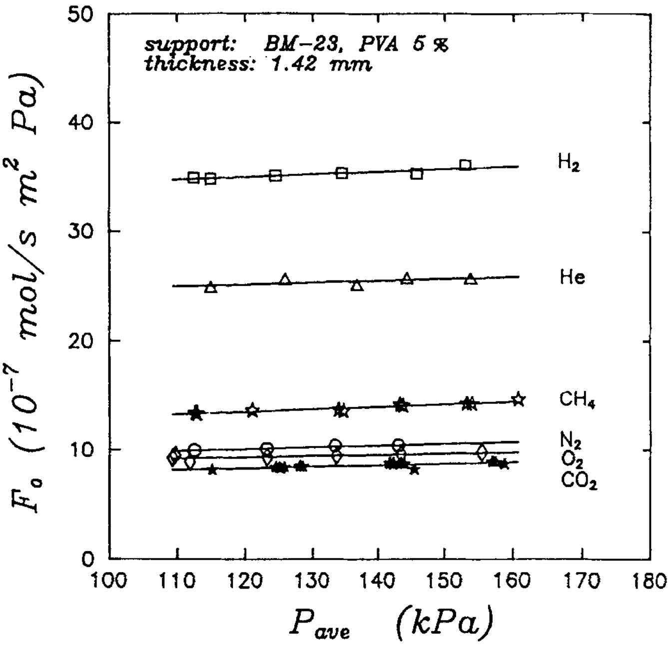

FIG. 9 Plot of F_0 vs P_{ave} at 26.5°C through the support prepared with 5% PVA.

ciencies. To this end, it is worthwhile to obtain representative values for the pore sizes which really contribute to the permeability.

For the calculation of pore size from mercury porosimetry, different techniques led to different results since the porous supports do not have uniform parallel cylindrical pores. There was a small portion of large pores in the 20–200 μm range, as shown in Fig. 4. As indicated in Table 2, the values of average pore diameters calculated by $\int d\, dV/\int dV$ were much larger than those calculated by $4V/A$. It can be seen that the values calculated by $4V/A$ were not strongly affected by the portion of large pores, while the values determined by $\int d\, dV/\int dV$ were strongly under the influence of large pores. In fact, large pores dominate the transport properties and the performance of porous supports. From the results of gas permeation measurements, the average diameters of active pores were roughly in agreement with those calculated from $\int d\, dV/\int dV$. Consequently, the average diameters of pores represented by $\int d\, dV/\int dV$ seem more relevant than those determined by $4V/A$.

Once the values of the average radii were determined, the porosity–tortuosity factors of these supports can be estimated from Eqs. (4) and (5). The tortuosity factors estimated from the values of porosity obtained by

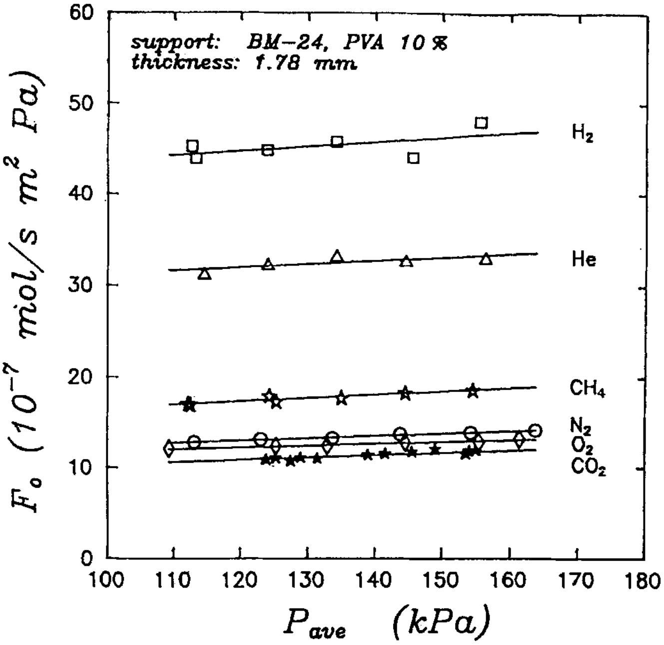

FIG. 10 Plot of F_0 vs P_{ave} at 26.5°C through the support prepared with 10% PVA.

TABLE 1
The Results of Gas Permeation through Various Supports at 26.5°C

Support	Gas	$F_{0K} \times 10^7$ (mol/s·m²·Pa)	$F_{0P} \times 10^{12}$ (mol/s·m²·Pa²)
BM-26, PVA 1%	H_2	26.975	3.575
	He	19.094	2.334
	CH_4	10.630	1.818
	N_2	8.264	0.986
	O_2	7.180	1.144
	CO_2	6.748	0.815
BM-23, PVA 5%	H_2	32.145	2.328
	He	23.064	1.729
	CH_4	10.763	2.262
	N_2	8.138	1.600
	O_2	8.033	1.064
	CO_2	6.667	1.364
BM-24, PVA 10%	H_2	38.744	5.045
	He	27.549	3.705
	CH_4	12.864	3.721
	N_2	9.899	2.574
	O_2	9.702	2.092
	CO_2	7.667	2.639

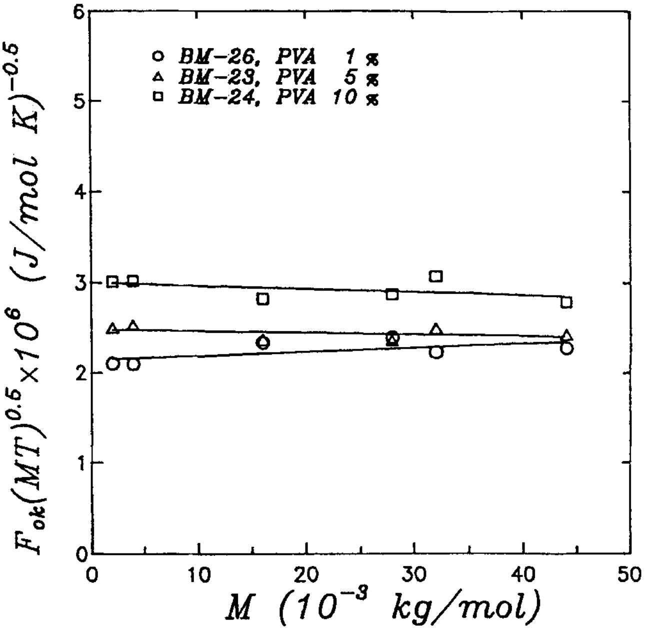

FIG. 11 Plot of $F_{0K}\sqrt{MT}$ vs M for various supports.

mercury porosimetry are shown in Table 2. Since the paths of the pores inside the supports are frequently tortuous, the tortuosity factors for the supports are thus much larger than unity. However, pores with dead ends do not contribute to the transport properties of the support, and the porosity obtained from mercury intrusion measurement does not distinguish through-pores and dead-pores. Therefore, the value of the tortuosity fac-

TABLE 2
The Average Pore Diameters, Porosity–Tortuosity Factors, and Tortuosity Factors for Various Supports

	Mercury porosimetry			Gas permeability method		
Support	ϵ (%)	d_{ave} (= $4V/A$) (μm)	d_{ave}[a] (μm)	d_{ave} (μm)	ϵ/τ (—)	τ (—)
PVA 1%	31.8	0.05	1.71	1.59	0.00982 ± 0.00060	32.5 ± 2.0
PVA 5%	35.1	0.08	1.77	1.52	0.01240 ± 0.00034	28.3 ± 0.8
PVA 10%	39.8	0.09	2.37	2.39	0.01178 ± 0.00039	33.9 ± 1.1
From γ-Al_2O_3	58.5	0.12	3.06	4.99	0.03397 ± 0.00751	30.2 ± 5.2

[a] $d_{ave} = \int d\,dV/\int dV$.

tor itself is not very meaningful, and the average radii of the "active" pores and porosity–tortuosity factors may be used instead as the main parameters to characterize the pore structure of a porous medium.

Besides, the average pore diameters and the values of tortuosity factors for the three supports are so close that the pore structures certainly have no obvious differences among them. In other words, the pore structure was not significantly affected by PVA amounts used in the preparation of the supports.

Comparison of Properties between Alumina Supports Prepared from α-Al_2O_3 and γ-Al_2O_3 Powders

The α-phase was obtained after the firing process for the two supports prepared from α-Al_2O_3 and γ-Al_2O_3 powders, respectively, and was confirmed by x-ray diffraction, as shown in Fig. 12. Pore size distribution for

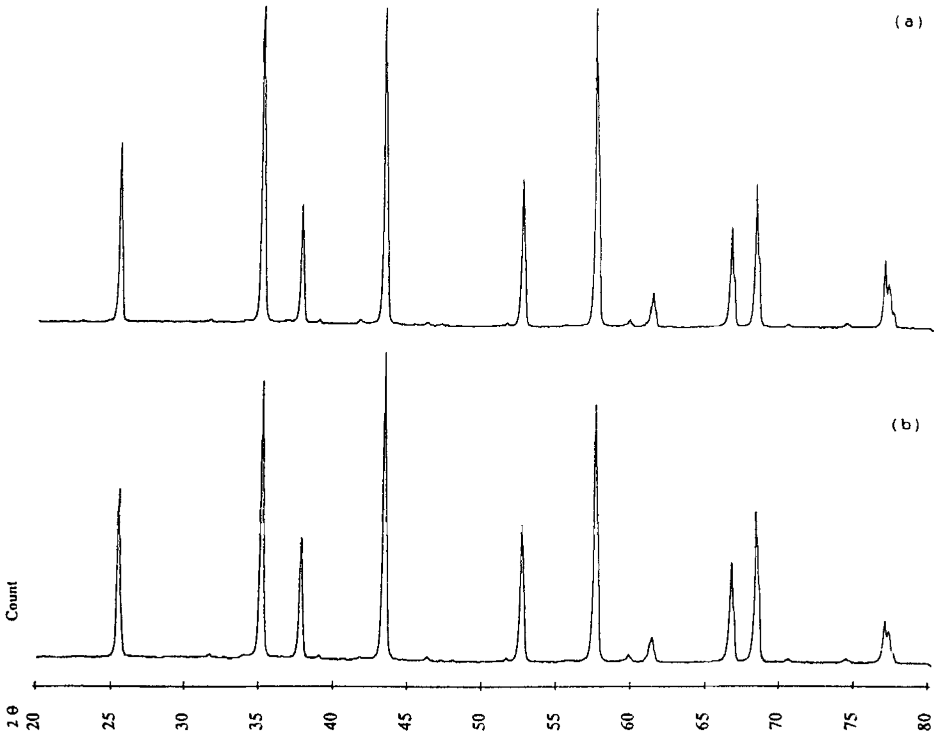

FIG. 12 XRD pattern for the supports prepared from (a) α-Al_2O_3 powder and (b) γ-Al_2O_3 powder.

the support prepared from γ-Al_2O_3 powders is also shown in Fig. 4. The pore size of the support prepared from γ-Al_2O_3 powders seems somewhat larger than those prepared from α-Al_2O_3 powders, and the porosity value of 58.5% was the highest among the four supports, as shown in Table 2 and Fig. 7(e). The permeability of gases through the support prepared from γ-Al_2O_3 powders was therefore much larger than the permeabilities through the supports prepared from α-Al_2O_3 powders. However, in Table 2, which indicates the tortuosity factors for the four supports, they do not show any considerable difference. Therefore, except for the pore size, the "pore pathways" of the supports prepared from γ-Al_2O_3 can be considered to be similar to those of the supports prepared from α-Al_2O_3.

Estimation of Ideal Separation Factors from the Permeabilities of Pure Gases

The ideal separation factor for a binary gaseous mixture can be determined from the ratio of permeabilities for the two gases, i.e., $\alpha_{ij}^* = F_{0,i}/F_{0,j}$. The ideal separation factors for the mixtures H_2/CH_4, H_2/CO_2, N_2/O_2, CH_4/CO_2, He/N_2, He/CO_2, and N_2/CO_2 are listed in Table 3. The theoretical ratios of permeabilities for binary mixtures in the Knudsen regime were calculated by using the inverse of the square root of the ratio of the molar masses of the two gases as seen in Eq. (6). The experimental values of ideal separation factors were somewhat lower than the theoretical ones for most of the mixtures due to the contribution of nonseparative Poiseuille permeation. Nevertheless, it appears that the experimental values of α_{ij}^* are in good agreement with the theoretical ones predicted by the Knudsen mechanism. Therefore, the results indicate that Knudsen diffusion was predominant for gas transport through the porous supports

TABLE 3
The Ideal Separation Factors for Binary Gaseous Mixtures at 26.5°C

	Gas													
	H_2/CH_4		H_2/CO_2		N_2/O_2		CH_4/CO_2		He/N_2		He/CO_2		N_2/CO_2	
P_{ave} (kPa)	100	160	100	160	100	160	100	160	100	160	100	160	100	160
PVA 1%	2.45	2.42	3.88	4.06	1.11	1.09	1.58	1.68	2.32	2.32	2.83	2.84	1.17	1.22
PVA 5%	2.65	2.48	4.29	4.05	1.10	1.09	1.62	1.64	2.55	2.41	3.09	2.92	1.21	1.21
PVA 10%	2.64	2.49	4.34	3.88	1.06	1.07	1.65	1.56	2.51	2.39	3.03	2.82	1.24	1.16
α_{ij}^*(Knudsen)[a]	2.82		4.67		1.07		1.66		2.65		3.32		1.25	

[a] Estimated from Eq. (6).

studied, and the porous supports alone provide considerable ability for separation.

CONCLUSIONS

1. The amount of PVA plays an important role in the preparation of porous alumina supports. The experimental results show that the surface area, pore size, and pore size distribution of a porous support do not vary to any significant extent with the amount of PVA used, but the pore volume and porosity increase with an increase in PVA dosage.

2. Transport through the alumina supports for H_2, He, CH_4, N_2, O_2, and CO_2 under low transmembrane pressure and room temperature can be considered to be in the transition regime where Knudsen diffusion and Poiseuille flow are both operative. The permeation results also show that the Knudsen mechanism is predominant.

3. The ideal separation factors determined from the permeabilities of pure gases for several mixtures show that the separation efficiencies are mainly limited by Knudsen diffusion and are in agreement with theoretical predictions.

4. The pore structure of alumina supports can be elucidated from gas permeation measurements along with mercury porosimetric analysis. It seems that the tortuosity factors for various porous supports are not appreciably affected by variation in the amount of PVA used. Except for porosity, the pore structure is almostly invariant within 0.5–10% of PVA addition in the preparation of porous supports. Consequently, addition of PVA is a powerful technique for controlling the porosity without affecting other microstructural properties significantly in the preparation of alumina supports. The "pore pathways" of supports prepared from γ-Al_2O_3 can be considered to be similar to those prepared from α-Al_2O_3.

NOMENCLATURE

A	pore area (m^2/g)
d	pore diameter (m)
F_0, $F_{0,i}$, $F_{0,j}$	gas permeability ($mol \cdot m/m^2 \cdot s \cdot Pa$)
F_{0K}	Knudsen permeability ($mol/m^2 \cdot s \cdot Pa$)
F_{0P}	Poiseuille permeability ($mol/m^2 \cdot s \cdot Pa^2$)
J	gas flux ($mol/m^2 \cdot s$)
Kn	Knudsen number (—)
l	thickness of the porous medium (m)
M, M_i, M_j	molar mass of the gas (kg/mol)
P_{ave}	average pressure (Pa)

ΔP	transmembrane pressure (Pa)
R	gas constant (J/mol·K)
r	pore radius (m)
T	temperature (K)
V	pore volume (cm^3/g)
α_{ij}^*	ideal separation factor for an ij mixture (—)
η	viscosity of a gas (Pa·s)
ϵ	porosity (—)
τ	tortuosity (—)
λ	mean free path for gas transport through a porous medium (m)

ACKNOWLEDGMENT

This work was performed under the auspices of the National Science Council of the Republic of China, under contract NSC82-0402-E006-085. The authors wish to express their thanks.

REFERENCES

1. T. A. Smith, *Trans. Br. Ceram. Soc.*, *61*, 523 (1962).
2. B. E. Yoldas, *Ceram. Bull.*, *54*(3), 289 (1975).
3. B. E. Yoldas, *J. Mater. Sci.*, *10*, 1856 (1975).
4. A. F. M. Leenaars, K. Keizer, and A. J. Burggraaf, *Ibid.*, *19*, 1077 (1984).
5. M. A. Anderson, M. J. Gieselmann, and Q. Xu, *J. Membr. Sci.*, *39*, 243 (1987).
6. H. P. Hsieh, *AIChE Symp. Ser.*, *84*(261), 1 (1988).
7. A. Larbot, J. P. Fabre, C. Guizard, and L. Cot, *J. Membr. Sci.*, *39*, 203 (1988).
8. V. T. Zaspalis, W. V. Praag, K. Keizer, J. R. H. Ross, and A. J. Burggraaf, *J. Mater. Sci.*, *27*, 1023 (1992).
9. R. R. Bhave (Ed.), *Inorganic Membranes: Synthesis, Characteristics, and Applications*, Van Nostrand Reinhold, New York, 1991.
10. W. E. Hauth Jr., *J. Am. Ceram. Soc.*, *32*(12), 394 (1949).
11. C. N. Satterfield, *Mass Transfer in Heterogeneous Catalysis*, Massachusetts Institute of Technology, Cambridge, Massachusetts, 1970.
12. F. P. Cuperus, and C. A. Smolders, *Adv. Colloid Interface Sci.*, *34*, 135 (1991).
13. D. E. Fain, in *Proc. 1st Int. Conf. Inorg. Membr.* (L. Cot and J. Charpin, Eds.), Refion Lanquedoc Roussilon, Montpellier, France, 1989, p. 199.
14. F. P. Cuperus, D. Bargeman, and C. A. Smolders, *J. Membr. Sci.*, *71*, 57 (1992).
15. A. Mey-Marom and M. G. Katz, *Ibid.*, *27*, 119 (1986).
16. H. Yasuda and J. T. Tsai, *J. Appl. Polym. Sci.*, *18*, 805 (1974).
17. F. W. Altena, H. A. M. Knoef, H. Heskamp, D. Bargememan, and C. A. Smolders, *J. Membr. Sci.*, *12*, 313 (1983).
18. Y. S. Lin and A. J. Burggraaf, *Ibid.*, *79*, 65 (1993).
19. S. T. Hwang and K. Kammermeyer, *Membrane in Separations, Vol. 7*, Wiley, New York, 1975.
20. R. R. Remick and J. Geankoplis, *Ind. Eng. Chem., Fundam.*, *12*(2), 214 (1973).

21. P. G. Carman, *Flow of Gases through Porous Media*, Butterworths, London, 1956.
22. K. Keizer, R. J. R. Uhlorn, R. J. Van Vuren, and A. J. Burggraaf, *J. Membr. Sci.*, *39*, 285 (1988).
23. J. C. S. Wu, D. F. Flowers, and P. K. T. Liu, *Ibid.*, *77*, 85 (1993).
24. K. Haraya, Y. Shindo, T. Hakuta, and H. Yashitome, *J. Chem. Eng. Jpn.*, *19*(3), 186 (1986).
25. A. F. M. Leenaars and A. J. Burggraaf, *J. Colloid Interface Sci.*, *105*(1), 27 (1985).
26. M. Robinson, J. A. Pask, and D. W. Fuerstenau, *J. Am. Ceram. Soc.*, *47*(10), 516 (1964).
27. W. E. Hauth Jr., *J. Phys. Colloid Chem.*, *54*, 142 (1950).
28. M. D. Sacks and T. Y. Tseng, *J. Am. Ceram. Soc.*, *66*(4), 242 (1983).
29. G. Lichti, R. G. Gilbert, and D. H. Napper, *J. Polym. Sci., Polym. Chem. Ed.*, *21*, 269 (1983).
30. Th. F. Tadros (Ed.), *Solid/Liquid Dispersions*, Academic Press, HBJ Publishers, London, 1987.
31. G. Y. Onoda Jr., in *Ceramic Processing before Firing* (G. Y. Onoda Jr. and L. L. Hench, Eds.), Wiley-Interscience, New York, 1978, p. 235.

Received by editor February 28, 1994
First revision received July 8, 1994
Second revision received July 28, 1994